Lab on a Chip

RSC Publishing

PAPER

View Article Online
View Journal | View Issue

Temperature-driven self-actuated microchamber sealing system for highly integrated microfluidic devices†

Cite this: *Lab Chip*, 2013, **13**, 452

Toyohiro Naito,*[a] Rerngchai Arayanarakool,[b] Séverine Le Gac,[b] Takao Yasui,[a] Noritada Kaji,[a] Manabu Tokeshi,[ac] Albert van den Berg[b] and Yoshinobu Baba[ad]

Received 11th September 2012,
Accepted 27th November 2012

DOI: 10.1039/c2lc41030c

www.rsc.org/loc

We present here a novel microchamber sealing valve that is self-actuated by a pressure change during the temperature change in the thermal activation of reactions. Actuation of our valve requires only the use of the same heating device as employed for the reactions. A thermoplastic UV-curable polymer is used as a device material; the polymer allows realization of the temperature-driven valve actuation as well as the fabrication of multi-layered devices. The self-actuated valve achieves effective sealing of the microchamber for the polymerase chain reaction (PCR) even at 90 °C, which is essential for developing highly parallel PCR array devices without the need for complicated peripherals to control the valve operation.

Introduction

Many integrated microdevices for genetic analytical processes have been developed. These devices have complicated channel designs as they carry out several procedures and functions.[1–3] One of the most fundamental and important elements in highly integrated lab-on-a-chip systems is a microfluidic valve technique to control the fluid flow.[4,5] In particular, for heating processes to activate chemical and biological reactions, valves are required that can seal the reaction mixture in a microreactor and prevent evaporation of the fluids.[6] For this reason, various strategies to develop microvalves for microfluidic PCR chips have been reported so far.

Several groups have reported a pneumatic microvalve composed of three layers for a main channel, a thin membrane and a valve control channel.[7–9] When pneumatic pressure is applied to the control channel, the membrane bends into the fluidic channel. This type of valve has been commonly used in many different microfluidic devices because it has a simple structure that is easily fabricated using soft lithography techniques and it can be controlled by a simple operation with versatile pumps. Furthermore, many valves have been derived from it, including normally closing microvalves,[8,10,11] valves using semi-round microchannels[12,13] and multiplex valves,[14–16] and they have all shown good performances, including zero back pressure, high integration, and high resistance to chemical corrosion. However, the valves require a great number of valve control channels which makes the designs of microdevices more complicated and larger. External pumps are also needed to actuate the valves.

Other developed valves are screw valves[17–19] and pinch-type valves.[20–22] The screw valves contain screws introduced above the microfluidic channels and the valves work by converting torque to vertical motion. The valve actuation can be controlled by changing the rotation angle and direction. Pinch-type valves have plungers to flatten out the microfluidic channels. The actuating mechanism and structure of pinch-type valves are similar to those of screw valves, but simpler and more compact. Pinch-type valves are able to actuate electromagnetically[17,20,21,23] due to their simple and compact structure. Electromagnetic microvalves often use a solenoid actuator with a magnetic core and a coil for generating the magnetic field that is converted to mechanical force for actuating valves. These valves are able to embed and actuate individually. Flow rates are programmable and can be controlled proportionally at a constant inlet pressure. Such individual integration and control should allow more complicated microfluidic control and procedures to be implemented in the microdevices. Although they have many advantages, external devices, such as solenoid actuators, electrodes and

[a]*Department of Applied Chemistry, Graduate School of Engineering, Nagoya University, FIRST Research Center for Innovative Nanobiodevices, Furo-cho, Chikusa-ku, Nagoya 464-8603, Japan. E-mail: naito.toyohiro@f.mbox.nagoya-u.ac.jp; Fax: +81 52 7894666; Tel: +81 52 7893560*
[b]*BIOS, The Lab-on-a-Chip Group, MESA+ Institute for Nanotechnology, University of Twente, Enschede, The Netherlands*
[c]*Division of Biotechnology and Macromolecular Chemistry, Faculty of Engineering, Hokkaido University, Kita 13 Nishi 8, Kita-ku, Sapporo 060-8628, Japan*
[d]*Health Research Institute National Institute of Advanced Industrial Science and Technology (AIST), Hayashi-cho 2217-14, Takamatsu 761-0395, Japan*

† Electronic supplementary information (ESI) available: Comparisons of optical properties, fabrication scheme of the NOA 81-based multilayer device, definition of the channel area, derivation of the equation of the elastic curve, independence of membrane deflection on the volume of a pneumatic chamber and valve-opening and -closing operations during thermal cycling. See DOI: 10.1039/c2lc41030c

circuits, are required for their control other than just the temperature control system used for chemical and biological reactions. These devices and structures do not just complicate the fabrication and the operation, but they also limit the integration level of the microchip.

Thermo-pneumatic valves and pumps have been developed using temperature-sensitive materials so that the valves are actuated effectively by temperature.[24–26] These temperature-sensitive materials could be adopted in microreactors using thermal activation for reactions to close the microreactors automatically, but putting a temperature-sensitive material into a microchannel involves cumbersome fabrication procedures.

In recent years, UV-curable polymer-based microfluidic devices have been reported as an alternative to poly(methyl methacrylate) (PMMA) or poly(dimethylsiloxane) (PDMS) and they were expected to be used for commercial prototype devices, because of their good mechanical properties, optical properties and very short curing time.[27,28] It was also reported that the glass transition temperatures of these UV-curable polymers were low.[28,29] In this paper, using a UV-curable polymer with a low glass transition temperature (around 40 °C) and structural mechanics theory, we developed a self-actuated sealing valve for a microreactor (Fig. 1).

Experimental

Material for the self-actuated sealing valve

A UV-curable adhesive, Norland Optical Adhesive 81 (NOA 81) (Norland Products Inc., Cranbury, NJ), was used to construct the self-actuated sealing valve. NOA 81 has been used for microfluidic channels[30–32] and as an intermediate layer in hybrid devices[33–35] because of the following advantages: (i) its surface affinity for water is easily changed using additives; (ii) it has high visible transmittance;[36] and (iii) it can be cured by UV irradiation within a short time (a few minutes or even seconds) under standard ambient conditions.

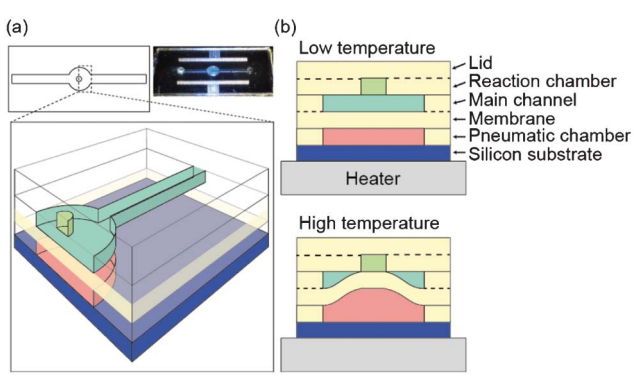

Fig. 1 (a) Structural drawing of our self-actuating microvalve. It consists of six layers, beginning at the top: a lid, reaction chamber, main channel, membrane, pneumatic chamber, and silicon substrate. (b) Cross-sections describing the working principle. Although this valve is normally open (top), the membrane bends into the main channel and closes the reaction chamber due to expansion of the pneumatic chamber caused by the temperature increase.

Operating principle

The chamber sealing system consists of thin multiple layers, including a reaction chamber, main channel, thin membrane acting as the valving element, and a pneumatic chamber used as a valve actuator; these are shown in Fig. 1a and c. A large area in the main channel is occupied by the cylindrical reaction chamber, and the circularly shaped pneumatic chamber fits into this large area. The membrane bends into the main channel and tightly seals the reaction chamber when the device is heated using a temperature controlled system due to expansion of the pneumatic chamber. A thermoplastic polymer was used as the device material to activate the valve at high temperature; this allows us to access the pneumatic chamber without using a thermal sensitive fluid or complicated fabrication procedure that replaces air with the fluid.

Fabrication

The NOA 81-based microfluidic and pneumatic layers used in this work were fabricated using a combination of UV-exposure and a casting technique for a PDMS-based mould (Fig. 2 and Fig. S1, ESI†). Standard photolithography techniques were used to fabricate SU-8-based moulds on silicon substrates [Fig. 2i, ii and Fig. S1, ESI† (1)]. The negative photoresist SU-8 50 (Microchem, Tokyo) was used to obtain a 50 μm resist layer for all layers. Subsequently the PDMS replicas were used for the NOA 81 casting. The NOA 81 is cured by UV irradiation, however, the surfaces of the NOA 81 sheets in contact with PDMS remained sticky due to oxygen in the PDMS moulds inhibiting the curing reaction. The sticky surfaces of NOA 81 were advantageous to bond other sheets. The reason why PDMS is used as a material for moulds is that PDMS has a high gas permeability, high UV transmittance and is commonly used for microfluidic devices.

A two-component kit (Sylgard 184, Dow Corning, Tokyo), including a pre-polymer of PDMS and curing agent, was used for PDMS fabrication; both were mixed in a 10 : 1 weight ratio. The resulting mixture was thoroughly degassed in a vacuum, poured into the silicon-SU8 mould, and degassed in a vacuum and cured for 2 h at 60 °C. The resulting chips were subsequently cleaned in ethanol in an ultrasonic bath for 15 min and carefully dried using compressed air before being used for the channel fabrication [Fig. 2 iii, iv, Figs. S1, ESI† (2) and (3)].

Three sets of interspaces were made, in which NOA sheets are used for the lid layer and the reaction chamber layer, the membrane layer and main channel layer, and the pneumatic chamber layer [Fig. 2S (4)†]. As for the bottom layer, a silicon substrate was used because of its thermal conductivity and reduced background signal during fluorescent observation. The UV-curable adhesive, NOA 81 precursor was injected and allowed to spread out slowly into the interspaces by capillary action prior to a 90 s curing step by UV irradiation [Fig. 2v, vi, Figs. S1, ESI† (5) and (6)]. A handy UV-light (As one, Osaka) with 1.65 mW cm^{-2} UV illumination at 365 nm was used to cure the adhesive, whereas the surfaces of the NOA 81 sheets remained sticky due to the reaction inhibition by oxygen. The PDMS moulds for the pneumatic chamber and membrane were peeled from the formed NOA 81 sheets and the two NOA

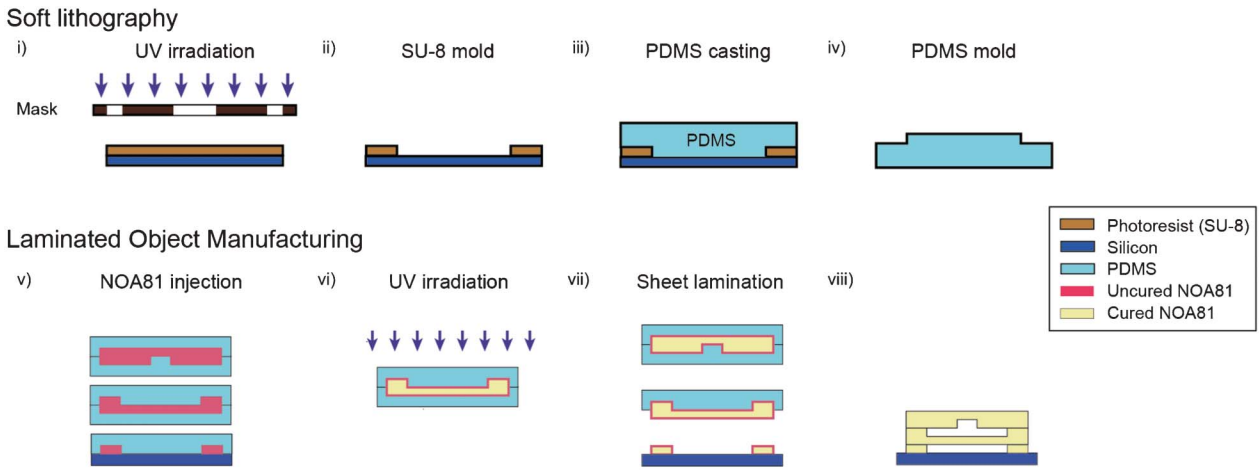

Fig. 2 Flow diagram of the fabrication procedures. Soft lithography techniques are combined with laminated object manufacturing techniques. PDMS moulds for making NOA sheets were fabricated by conventional soft lithography (i–iv). NOA 81 was injected into the interspaces of the PDMS moulds, and cured by UV irradiation. The curing reaction of the surfaces in contact with PDMS moulds was inhibited by oxygen present in the PDMS moulds. Finally, the NOA sheets were laminated and bonded through the action of the sticky uncured surfaces.

81 sheets were bonded by UV irradiation for 30 s. Two access holes for sample introduction were made in the NOA 81 sheet used for the lid after peeling off the two PDMS moulds for the lid. Finally, the PDMS mould for the main channel on the NOA sheets bonded to the silicon substrate was peeled off, and the assembled NOA sheets were laminated and bonded by UV irradiation for 3 min [Fig. 2vii, viii, Figs. S1, ESI† (7) and (8)].

Evaluation of the valve function

The chip main channel was filled with an aqueous solution of 0.5 mM fluorescein sodium salt (Sigma–Aldrich, Tokyo) and placed on a peltier heater that was computer-controlled with a proportional integral derivative (PID) control algorithm. The thermal control system was comprised of a power supply (HLE, Nihontecmo Co. Ltd., Fukuoka, Japan), a controller (SP5R7-576, Nihontecmo Co. Ltd.), a thermocouple (SPTS67-170, Nihontecmo Co. Ltd.), a peltier module (TEC-12708, Nihontecmo Co. Ltd) and LabVIEW-based control and data-logging software.

Fluorescence images of the channel above the pneumatic chamber were captured with temperature changes using a camera (e-420, Olympus, Tokyo) mounted on a fluorescent microscope (AZ-100, Nikon, Tokyo) with a light beam from a mercury lamp and B-2A filter set (Nikon, Tokyo). The fluorescence intensity was measured with open source image analysis software (ImageJ).

Results and discussion

Proof of concept

The valve was designed to actuate thermally utilizing the thermoplastic material NOA 81. To confirm the principle of operation, we studied the softening of a NOA sheet while increasing the temperature. A NOA sheet (10 mm × 20 mm × 50 μm) was fabricated by the same process using the PDMS mould for the membrane layer and a flat PDMS stamp. The NOA sheet was put on one side of a heater so that it stuck out 1 cm beyond the heater; a weight was set on the sheet and the sheet was observed from the side as shown in Fig. 3. The sheet dramatically softened above 40 °C, enough to deform under its own weight, whereas it did not deform at temperatures up to 31 °C. This result was a reflection of the low glass-transition temperature of the NOA 81. The Young's modulus of NOA 81 at 83 °C was roughly estimated as 5 MPa using the beam deflection formula for a cantilever beam under a uniformly distributed load.[37] The value is two orders of magnitude less than the value at 25 °C (1400 MPa in a previous report[27]).

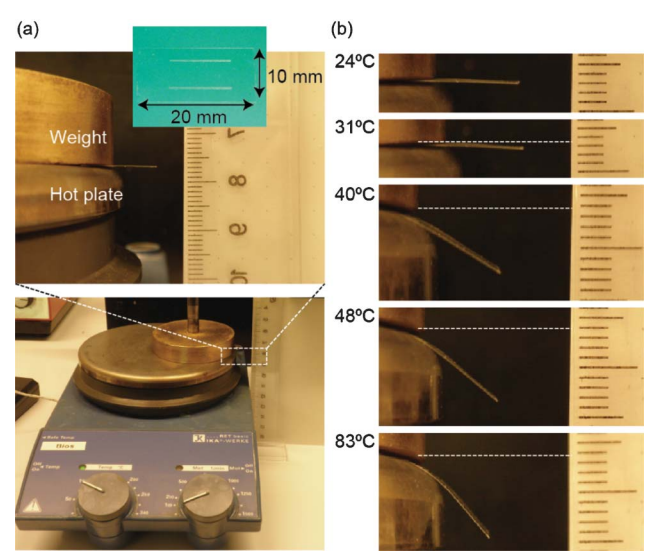

Fig. 3 (a) Photographs of the simplified equipment for measuring the Young's modulus change at various temperatures. A NOA 81 sheet (10 mm × 20 mm × 50 μm) was clamped between a hotplate and a weight. (b) Bending of the NOA sheet due to the Young's modulus change with temperature increase.

Although the flexibility of NOA 81 is a little higher than that of PDMS (0.5–2.5 MPa),[38,39] we consider that the true value is lower than the calculated result due to the rounded edge of the heater and having some unheated part of the sheet.

We demonstrated the valve function using a straight main channel without a reaction chamber (Fig. 4). The fluorescent solution was clearly found in the channel at 25 °C, however, the fluorescent intensity became gradually lower with an increase in temperature (Fig. 4a). This meant that the valve completely closed the channel at high temperatures, except near the sidewall. We also confirmed that the device is a repeatable valve as seen in the movie S1, ESI.† The valve repeated closing and opening operations during five repeated temperature cycles (95 °C for 30 s, 75 °C for 30 s, 55 °C for 30 s) (Fig. 4b). The mean of the fluorescence intensity at the valve was changed in response to the temperature changes due to increasing pressure in the closing part (Fig. 4). The valve could be used over and over again during thermal cycling for more than 20 min.

Valve characterization

Cross-sectional shapes of the membrane deflection were estimated from the fluorescence images of the fluorescein-filled microchannel to characterize the valve functions. The cross-section information gives an area where the membrane deflection $\delta(x)$ is larger than the original channel depth d_0, the area is useful for designing reaction chamber sealing devices (Fig. 5a). Normal straight channels were used for investigating the relationships of various parameters. The measured fluorescence intensity represents a channel depth at an arbitrary point after membrane bending. The membrane deflection can be calculated using the bending theory for a thin plate with all edges fixed under uniformly distributed loads. It is reasonable to assume that the fluorescence intensities near the side channel walls mean the original channel depth, because thin plate deflection at fixed edges equals 0. The side channel walls in the fluorescence images were defined using an edge detection method with second-order derivative approaches (see ESI†).

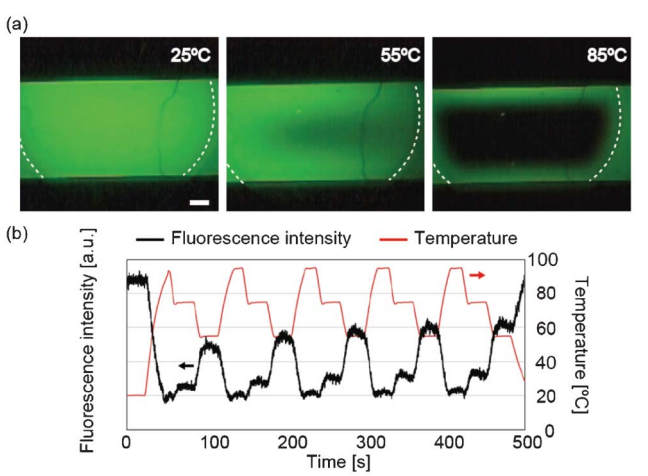

Fig. 4 (a) Fluorescence images obtained at 25 °C, 55 °C and 85 °C for the thermo-pneumatic valve with the normal straight channel. White dotted lines show pneumatic chambers. Scale bar, 200 μm. (b) Change of fluorescence intensity at the valve during thermal cycling (95 °C for 30 s, 75 °C for 30 s, 55 °C for 30 s). The red and black lines represent the measuring device temperature and average of the fluorescence intensity at the valve, respectively.

We used the theoretical curve to evaluate and compare quantitatively the valve function under different conditions as illustrated in Fig. 5b. A thin rectangular plate with fixed edges was regarded as a continuum of bars that were vertical structural elements with both ends fixed; this was done to simplify solving the equation of the elastic curve for the thin plate. According to structural mechanics, deflection of a beam fixed at both ends under a uniformly distributed load[37] can be calculated using eqn (1):

$$\delta(x) = \frac{wl^2x^2}{24EI}\left(1 - \frac{2x}{l} + \frac{x^2}{l^2}\right) \quad (1)$$

where $\delta(x)$ is the membrane deflection at position x, w is the load on the beam, and l is the channel width (Fig. 5b). E is the Young's modulus, I is the second moment of area given by $I = lh^3/12$ (h being the thickness of the membrane). The derivation of eqn (1) is described in the ESI.† For the membrane deflection evaluation parameter, we used the maximum value deflection, δ_C, which is the deflection value at the centre point [$\delta_C = \delta(l/2)$] as shown in Fig. 5b. When $l/2$ is substituted for x, eqn (2) follows from eqn (1):

$$\delta_C = \frac{wl^4}{384EI} \quad (2)$$

and eqn (3) is obtained from eqn (1) and (2).

$$\delta(x) = \frac{16\delta_C x^2}{l^2}\left(1 - \frac{2x}{l} + \frac{x^2}{l^2}\right) \quad (3)$$

Eqn (3) was used as a theoretical formula for curve fitting to the measured values by the least squares method. The coefficient of determination R^2 was used for evaluating the goodness of the fit of the values expected by eqn (3). Fig. 5c shows the curve fitting to measured values at 80 °C with a 200 μm wide channel. The theoretical curve approximated well the noisy measured data from the minimum to the maximum R^2 in this paper ($0.860 \leqslant R^2 \leqslant 0.972$).

For investigating the relationships of various parameters, we used the straight main channel with variations of the width (600, 800, 1000 μm). Fig. 5d illustrates the relationships between the temperature dependence and the physical dimensions of channel width of the membrane deflection at the centre point. Membrane deflection was increased with increases in device temperature and the channel width; it was proportional to the temperature and the fourth power of the channel width. Temperature dependence of membrane deflection agreed with Charles' law that describes the relationship of the temperature and volume of a gas, because w, the value of the uniformly distributed load, has the same meaning as pressure in one dimension. As for the channel width dependence, it was explained by eqn (1), which indicated the proportional relationship with the membrane deflection and the fourth power of the channel width (Fig. 5e). By contrast,

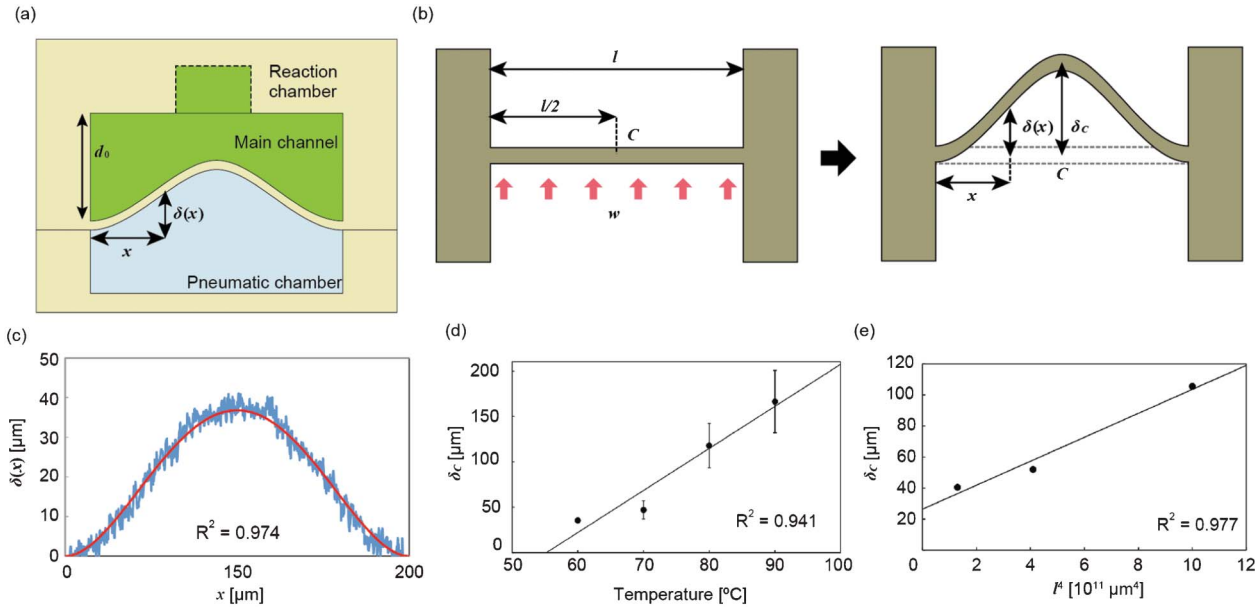

Fig. 5 (a) Schematic diagram of membrane bending in the channel as a cross-sectional view. The main channel was filled with fluorescein solution, and the fluorescence intensity indicates the effective channel depth after membrane bending into the main channel. (b) The model showing deflection of a beam fixed at both ends under a uniformly distributed load. δ_x is the membrane deflection at position x, w is the load on the beam, and l is channel width. C is the centre point of the beam and it has the largest deflection value. (c) Curve fitting of the measured data. Blue and red lines show the measurement data and a fitting curve, respectively. (d) The temperature dependence on membrane deflection. (e) The channel width dependence on a membrane deflection at 80 °C. The horizontal axis represents the fourth power of channel width.

the membrane deflection had no relationship with the depth of the pneumatic chamber (Fig. S4, ESI†). This was also consistent with the gas law; pressure is constant if the molecular volume of the gas is kept constant at the same temperature.

Microreactor sealing

Finally, we developed a chamber sealing system that encloses a solution within a reaction chamber using a heating device. A reaction chamber was fabricated on the completely closed area in a main channel by using a membrane. The channel width l was 2 mm and the channel depth d_0 was 50 μm, and the device parameters, δ_C at 80 °C and the diameter of the completely closed area, were expected to be 149 μm and 1.3 mm, respectively. We designed the reaction chamber to be 1 mm in diameter so that the membrane would seal up the reaction chamber. As expected, the self-actuated valve worked very well at high temperature and effectively sealed the reaction chamber for PCR at 80 °C, as shown in Fig. 6, which is in contrast to the situation at 25 °C, showing the presence of the fluorescent solution in the main channel with the reaction chamber. Although the membrane bent into the reaction chamber at temperatures higher than 70 °C when using the large diameter reaction channel, it was possible to determine the optimal physical dimensions of the channel based on eqn (1). We can improve the valve for actuation at lower temperatures by changing the Young's modulus, membrane thickness, channel depth and radius of the reaction chamber. Using a material that has a smaller Young's modulus and using a thinner membrane may enhance the membrane

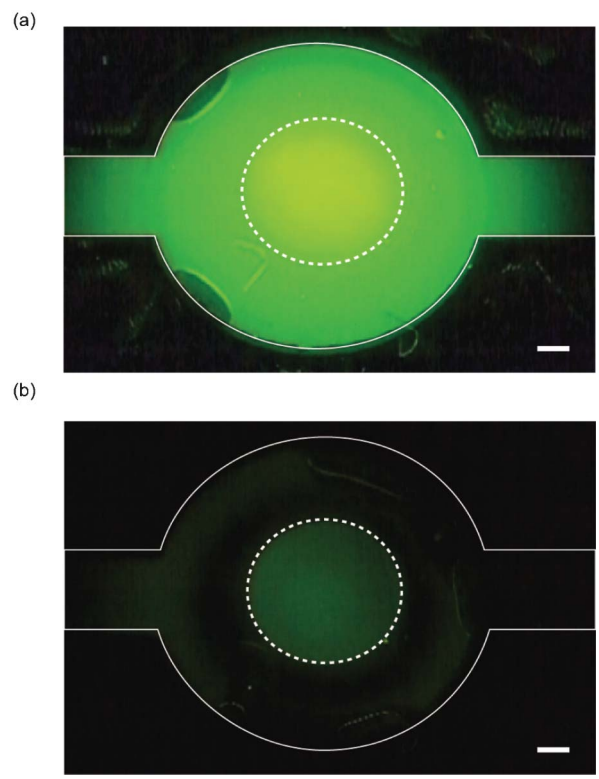

Fig. 6 Fluorescent images of the microchamber sealing device obtained at (a) 25 °C and (b) 80 °C. The outer white solid lines mark the main channel and the white dotted circles show the reaction chamber. Scale bars are 200 μm.

deflection because the membrane deflection is affected by the load, Young's modulus and membrane thickness according to eqn (1). In addition, a smaller radius reaction chamber and shallower channel makes it easier for the membrane to seal the reaction chamber.

Conclusions

The temperature-driven self-actuated microvalve provides effective sealing of a microreactor simultaneous to the heating process of the reaction. We fabricated the valve from a UV-curable adhesive to provide a tool that can bridge the gap between basic research in microfluids and commercialised products. The valve was actuated by the thermoplasticity of its NOA 81 membrane and expansion of an actuation chamber volume associated with increased temperature for the thermal activation of a reaction. Theoretical curve fitting revealed the deformed state of the membrane in a microchannel, and verified the relationships between membrane deflection, device temperature, and channel width.

This sealing device is suitable for PCR chips or chemical reaction chips, which require closed reaction chambers and the prevention of reaction liquid evaporation during a reaction process. This device will also be helpful for designing highly integrated microfluidic devices by featuring combined uses of micro heaters such as laser heating, ITO heaters, and micropeltier elements.

Acknowledgements

This research was partially supported by the Japan Society for the Promotion of Science (JSPS) through its ''Funding Program for World-Leading Innovative R&D on Science and Technology (FIRST Program)'', International Training Program (ITP), Institutional Program for Young Researcher Overseas Visits, and Grants-in-Aid for JSPS Fellows. This work was partly supported by Nanotechnology Platform Program (Molecule and Material Synthesis) of the Ministry of Education, Culture, Sports, Science and Technology (MEXT), Japan.

References

1 C. J. Easley, J. M. Karlinsey, J. M. Bienvenue, L. A. Legendre, M. G. Roper, S. H. Feldman, M. A. Hunghes, E. L. Hewlett, T. J. Merkel, J. P. Ferrance and J. P. Landers, *Proc. Natl. Acad. Sci. U. S. A.*, 2006, **103**, 19272–19277.
2 Y. Wang, W.-Y. Lin, K. Liu, R. J. Lin, M. Selke, H. C. Kolb, N. Zhang, X.-Z. Zhao, M. E. Phelps, C. K. F. Shen, K. F. Faull and H.-R. Tseng, *Lab Chip*, 2009, **9**, 2281–2285.
3 R. Pal, M. Yang, R. Lin, B. N. Jhonson, N. Srivastava, S. Z. Razzacki, K. J. Chomistek, D. C. Heldsinger, R. M. Haque, V. M. Ugaz, P. K. Thwar, Z. Chen, K. Alfano, M. B. Yim, M. Krishnan, A. O. Fuller, R. G. Larson, D. T. Burke and M. A. Burns, *Lab Chip*, 2005, **5**, 1024–1032.
4 R. Gómez-Sjöberg, A. A. Leyrat, D. M. Pirone, C. S. Chen and S. R. Quake, *Anal. Chem.*, 2007, **79**, 8557–8563.
5 C-C. Lee, G. Sui, A. Elizarov, C. J. Shu, Y.-S. Shin, A. N. Dooley, J. Huang, A. Daridon, P. Wyatt, D. Stout, H. C. Kolb, O. N. Witte, N. Satyamurthy, J. R. Heath, M. E. Phelps, S. R. Quake and H.-R. Tseng, *Science*, 2005, **310**, 1793–1796.
6 L. A. Christel, K. Petersen, W. McMillan and M. A. Northrup, *J. Biol. Eng.*, 1999, **121**, 22–27.
7 M. A. Unger, H. P. Chou, T. Thorsen, A. Schere and S. R. Quake, *Science*, 2000, **288**, 113–116.
8 G. Thuillier and C. K. Malek, *Microsyst. Technol.*, 2005, **12**, 180–185.
9 S.-I. Han, K.-H. Han, A. B. Frasier, J. P. Ferrance and J. P. Landers, *Biomed. Microdevices*, 2009, **11**, 935–942.
10 W. H. Grover, R. H. C. Ivester, E. C. Jensen and R. A. Mathies, *Lab Chip*, 2006, **6**, 623–631.
11 K. Hosokawaa and T. Maeda, *J. Micromech. Microeng.*, 2000, **10**, 415–420.
12 V. Studer, G. Hang, A. Pandolfi, M. Ortiz, W. F. Anderson and S. R. Quake, *J. Appl. Phys.*, 2004, **95**, 393–398.
13 W. Park, S. Han and S. Kwon, *Lab Chip*, 2010, **10**, 2814–2817.
14 T. Thorsen, S. J. Maerkl and S. R. Quake, *Science*, 2002, **298**, 580–584.
15 L. M. Fidalgo and S. J. Maerkl, *Lab Chip*, 2011, **11**, 1612–1619.
16 B. Mosadegh, H. Tavana, S. C. Lescher-Prez and S. Takayama, *Lab Chip*, 2011, **11**, 738–742.
17 S. E. Hulme, S. S. Shevkoplyas and G. M. Whitesides, *Lab Chip*, 2009, **9**, 79–86.
18 C.-F. Chen, J. Liu, C.-C. Chang and D. L. DeVoe, *Lab Chip*, 2009, **9**, 3511–3516.
19 D. B. Weibel, M. Kruthof, S. Potenta, S. K. Sia, A. Lee and G. M. Whitesides, *Anal. Chem.*, 2005, **77**, 4726–4733.
20 Y. Shinozawa, T. Abe and T. Kondo, *Proceedings of MEMS'97 10 th IEEE International Workshop micro Electromechanical system*, 1997, 233–237.
21 K. W. Oh. R. Rong and C. H. Ahn, *J. Micromech. Microeng.*, 2005, **15**, 2449–2455.
22 A. W. Browne, K. E. Hitchcock and C. H. Ahn, *J. Micromech. Microeng.*, 2009, **19**, 115012–115019.
23 T. Hasegawa, K. Nakashima, F. Omatsu and K. Ikuta, *Sens. Actuators, A*, 2008, **143**, 390–398.
24 S. Mutlu, C. Yu, F. Svec, C. H. Mastrangelo, J. M. M. Fréchet and Y. B. Gianchandani, *Proc. Transducers*, 2003, 802–805.
25 G. V. Kalgala, V. N. Hoang and C. J. Backhouse, *Lab Chip*, 2008, **8**, 1071–1078.
26 K. Pitchaimai, B. C. Sapp, A. Winter, A. Gispanski, T. Nishida and Z. H. Fan, *Lab Chip*, 2009, **9**, 3082–3087.
27 D. Bartolo, G. Degré, P. Nghe and V. Studer, *Lab Chip*, 2008, **8**, 274–279.
28 C. F. Carlborg, T. Haraldsson, K. Öberg, M. Malkoch and W. van der Wijngaart, *Lab Chip*, 2011, **11**, 3136–3147.
29 R. Benmouna and B. Benyoucef, *J. Appl. Polym. Sci.*, 2008, **108**, 4072–4079.
30 P. Wägli, A. Hosmy and N. F. de Rooij, *Sens. Actuators, B*, 2011, **156**, 994–1001.
31 X. Li, F. Zhang, L. Wang, J.-H. Tian, X.-T. Zhou, L.-M. Jiang, L. Liu, Z.-J. Zhao, P.-G. He and Y. Chen, *Electrophoresis*, 2011, **32**, 3201–3206.
32 Y. Zheng, W. Dai, D. Ryan and H. Wu, *Biomicrofluidics*, 2010, **4**, 036504–036514.

33 S. Schlautmann, G. A. J. Basselink, R. Prabhu and R. B. M. Schasfoort, *J. Micromech. Microeng.*, 2003, **13**, S81–S84.
34 Z. L. Huang, J. C. Sanders, C. Dunsmor, H. Ahmadsadeh and J.P. Landers, *Electrophoresis*, 2001, **22**, 3924–3929.
35 R. Arayanarakool, S. L. Gac and A. van den Berg, *Lab Chip*, 2010, **10**, 2115–2121.
36 Norland Products Inc., NOA 81, Norland Optical Adhesive 81, http://www.norlandproducts.com/adhesives/noa%2081.html, accessed August 2, 2012.
37 S. Timoshenko, *Strength of Materials*, D. Van Nostrand company Inc., New York, 1948, ch. 6, pp. 184–188.
38 X. Q. Brown, K. Ookawa and J. Y. Wong, *Biomaterials*, 2005, **26**, 3123–3129.
39 J. L. Tan, J. Tien, D. M. Pirone, D. S. Gray, K. Bhadriaju and C. S. Chen, *Proc. Natl. Acad. Sci. U. S. A.*, 2003, **100**, 1484–1489.

